Correction

MEDICAL SCIENCES

Correction for "The myokine irisin increases cortical bone mass," by Graziana Colaianni, Concetta Cuscito, Teresa Mongelli, Paolo Pignataro, Cinzia Buccoliero, Peng Liu, Ping Lu, Loris Sartini, Mariasevera Di Comite, Giorgio Mori, Adriana Di Benedetto, Giacomina Brunetti, Tony Yuen, Li Sun, Janne E. Reseland, Silvia Colucci, Maria I. New, Mone Zaidi, Saverio Cinti, and Maria Grano, which appeared in issue 39, September 29, 2015, of *Proc Natl Acad Sci USA* (112:12157–12162; first published September 15, 2015; 10.1073/pnas.1516622112).

The authors note that their conflict of interest statement was omitted during publication. The authors declare that G.C., C.C., G.M., G.B., S. Colucci, S. Cinti, and M.G. are named inventors of a pending patent application related to the work described.

www.pnas.org/cgi/doi/10.1073/pnas.1519137112

The myokine irisin increases cortical bone mass

Graziana Colaianni[a,1], Concetta Cuscito[a,1], Teresa Mongelli[a], Paolo Pignataro[a], Cinzia Buccoliero[a], Peng Liu[b], Ping Lu[b], Loris Sartini[c], Mariasevera Di Comite[a], Giorgio Mori[d], Adriana Di Benedetto[d], Giacomina Brunetti[a], Tony Yuen[b], Li Sun[b], Janne E. Reseland[e], Silvia Colucci[a], Maria I. New[b,2], Mone Zaidi[b,2], Saverio Cinti[c], and Maria Grano[a,2]

[a]Department of Basic Medical Science, Neuroscience and Sense Organs, University of Bari, 70124 Bari, Italy; [b]The Mount Sinai Bone Program, Departments of Medicine and Pediatrics, Mount Sinai School of Medicine, New York, NY 10029; [c]Department of Experimental and Clinical Medicine, Center of Obesity, United Hospitals, University of Ancona, 60020 Ancona, Italy; [d]Department of Clinical and Experimental Medicine, University of Foggia, 71100 Foggia, Italy; and [e]Department of Biomaterials, Institute for Clinical Dentistry, University of Oslo, Blindern, N-0317 Oslo, Norway

Contributed by Maria I. New, August 21, 2015 (sent for review May 21, 2015; reviewed by Christopher Huang and Carlos M. Isales)

It is unclear how physical activity stimulates new bone synthesis. We explored whether irisin, a newly discovered myokine released upon physical activity, displays anabolic actions on the skeleton. Young male mice were injected with vehicle or recombinant irisin (r-irisin) at a low cumulative weekly dose of 100 μg kg^{-1}. We observed significant increases in cortical bone mass and strength, notably in cortical tissue mineral density, periosteal circumference, polar moment of inertia, and bending strength. This anabolic action was mediated primarily through the stimulation of bone formation, but with parallel notable reductions in osteoclast numbers. The trabecular compartment of the same bones was spared, as were vertebrae from the same mice. Higher irisin doses (3,500 μg kg^{-1} per week) cause browning of adipose tissue; this was not seen with low-dose r-irisin. Expectedly, low-dose r-irisin modulated the skeletal genes, *Opn* and *Sost*, but not *Ucp1* or *Pparγ* expression in white adipose tissue. In bone marrow stromal cell cultures, r-irisin rapidly phosphorylated Erk, and up-regulated *Atf4*, *Runx2*, *Osx*, *Lrp5*, *β-catenin*, *Alp*, and *Col1a1*; this is consistent with a direct receptor-mediated action to stimulate osteogenesis. We also noted that, although the irisin precursor *Fndc5* was expressed abundantly in skeletal muscle, other sites, such as bone and brain, also expressed *Fndc5*, albeit at low levels. Furthermore, muscle fibers from r-irisin–injected mice displayed enhanced Fndc5 positivity, and irisin induced *Fdnc5* mRNA expression in cultured myoblasts. Our data therefore highlight a previously unknown action of the myokine irisin, which may be the molecular entity responsible for muscle–bone connectivity.

mechanical loading | sarcopenia | osteoporosis

Physical exercise has widely recognized benefits on metabolic and skeletal health, and is routinely used as a nonpharmacologic intervention in therapeutic protocols for a variety of diseases (1, 2). Decreases in the level of physical activity, for example in former athletes, can lead to progressive loss of bone (3). Likewise, disuse and weightlessness invariably cause acute, rapid, and severe bone loss with a profound increase in fracture risk (4). For example, astronauts lose bone mass 10 times faster than women in early menopause (5), whereas patients in a vegetative state or with spinal cord injuries display a high risk of fragility fractures, even at a low-normal bone mineral density (BMD) (6).

Although there is a clear link between physical activity and bone acquisition and maintenance, the question of whether and how muscle function regulates bone mass has remained largely unresolved. Several lines of evidence point toward direct muscle–bone connectivity. First, higher muscle mass appears closely related to a higher BMD and, consequently, reduced fracture risk in postmenopausal women. Conversely, age-related sarcopenia has been linked to senile osteoporosis (7). Second, glucocorticoid excess and vitamin D deficiency are catabolic, whereas androgens are anabolic to both bone and muscle (8, 9). Third, we find that, in rats with experimental spinal cord injury, electrical stimulation of muscle rescues the elevated bone resorption and osteoclastogenesis in vivo, in essence providing direct evidence for muscle–bone communication, likely through a soluble molecule (10).

The newly identified myokine irisin, produced by skeletal muscle in response to exercise, has recently drawn attention as a potential target for treating metabolic disorders (11). Overexpression of Pgc-1α in muscle during exercise has been shown to stimulate the production of the membrane protein fibronectin type III domain containing protein 5 (Fndc5). The latter is subsequently cleaved to, and released as, irisin (11). Irisin induces a "browning response" in white adipose tissue (WAT) (12–14), and triggers a transdifferentiation program wherein white adipocytes (15) or de novo beige/brite cells (14, 16) shift from a WAT to a brown adipose tissue (BAT)-like phenotype (11). These elegant studies have directly linked muscle function to obesity via a myokine.

We have shown previously that myokine-enriched medium from myoblast cultures was able to enhance the differentiation of bone marrow stromal cells into mature, bone-forming osteoblasts in vitro (17). Here, we demonstrate that recombinant irisin (r-irisin), when injected into mice, increases cortical bone mass and strength. We find that this action arises from a direct effect of irisin on osteoblastic bone formation, which is exerted mainly through the suppression of sclerostin (*Sost*), a Wnt signaling inhibitor. We believe that irisin may serve as a lead molecule toward the future development of novel therapies that might simultaneously target disorders of bone, muscle and metabolism.

Significance

Although exercise is a well known and potent stimulus for new bone formation, and weightlessness or muscle loss characteristically cause bone loss, it has remained unclear how muscle talks to bone, despite their close proximity. Here, we show that a molecule irisin derived from skeletal muscle in response to exercise has profound effects in enhancing mass and improving the geometry and strength specifically of cortical bone, the key function of which is to resist bending and torsion. Trabecular bone, which is a reservoir for bodily calcium, is remarkably spared. Irisin may therefore not only be the molecule responsible for muscle–bone connectivity, but could also become a therapy for sarcopenia and osteoporosis, which occur in tandem in the elderly.

Author contributions: C.C., S. Colucci, M.I.N., M.Z., S. Cinti, and M.G. designed research; G.C., T.M., P.P., C.B., P. Liu, P. Lu, L. Sartini, M.D.C., G.M., A.D.B., G.B., T.Y., and J.E.R. performed research; G.C., C.C., G.M., T.Y., L. Sun, J.E.R., S. Colucci, M.Z., S. Cinti, and M.G. analyzed data; and G.C., T.Y., M.I.N., M.Z., and M.G. wrote the paper.

Reviewers: C.H., University of Cambridge; and C.M.I., Georgia Regents University.

The authors declare no conflict of interest.

[1]G.C. and C.C. contributed equally to this work.

[2]To whom correspondence may be addressed. Email: mone.zaidi@mssm.edu, maria.new@mssm.edu, or maria.grano@uniba.it.

This article contains supporting information online at www.pnas.org/lookup/suppl/doi:10.1073/pnas.1516622112/-/DCSupplemental.

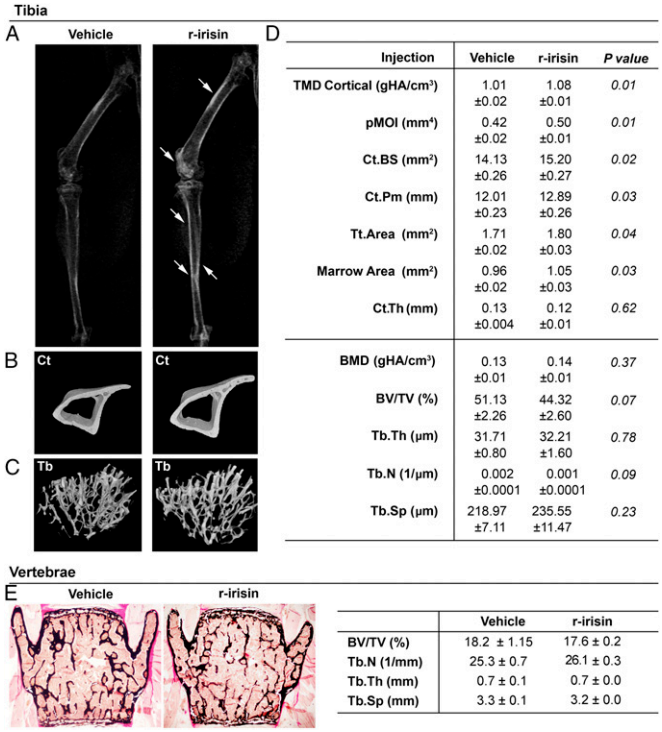

D

Injection	Vehicle	r-irisin	*P value*
TMD Cortical (gHA/cm³)	1.01 ±0.02	1.08 ±0.01	*0.01*
pMOI (mm⁴)	0.42 ±0.02	0.50 ±0.01	*0.01*
Ct.BS (mm²)	14.13 ±0.26	15.20 ±0.27	*0.02*
Ct.Pm (mm)	12.01 ±0.23	12.89 ±0.26	*0.03*
Tt.Area (mm²)	1.71 ±0.02	1.80 ±0.03	*0.04*
Marrow Area (mm²)	0.96 ±0.02	1.05 ±0.03	*0.03*
Ct.Th (mm)	0.13 ±0.004	0.12 ±0.01	*0.62*
BMD (gHA/cm³)	0.13 ±0.01	0.14 ±0.01	*0.37*
BV/TV (%)	51.13 ±2.26	44.32 ±2.60	*0.07*
Tb.Th (μm)	31.71 ±0.80	32.21 ±1.60	*0.78*
Tb.N (1/μm)	0.002 ±0.0001	0.001 ±0.0001	*0.09*
Tb.Sp (μm)	218.97 ±7.11	235.55 ±11.47	*0.23*

	Vehicle	r-irisin
BV/TV (%)	18.2 ± 1.15	17.6 ± 0.2
Tb.N (1/mm)	25.3 ± 0.7	26.1 ± 0.3
Tb.Th (mm)	0.7 ± 0.1	0.7 ± 0.0
Tb.Sp (mm)	3.3 ± 0.1	3.2 ± 0.0

Fig. 1. Anabolic action of low-dose recombinant irisin (r-irisin) on cortical bone. (*A*) Contact radiographs of selected long bones from mice treated with vehicle or low-dose r-irisin (100 μg kg^{-1} per week for 28 d, mice killed 24 h after last dose). Arrows indicate areas of increased radiodensity. Representative micro-CT–generated section images of cortical (midshaft, *B*) and trabecular (metaphyseal, *C*) bone in tibia harvested from vehicle- or irisin-injected mice. (*D*) Calculated cortical and trabecular parameters at the tibial midshaft and metaphysis of vehicle- or r-irisin–injected mice. Cortical bone parameters included tissue mineral density (TMD-Cortical), polar moment of inertia (pMOI), cortical bone surface (Ct.BS), cortical bone perimeter (Ct.Pm), total cross-sectional area (Tt.Area), marrow cross-sectional area (Marrow Area), and cortical thickness (Ct.Th). Trabecular bone parameters for tibial epiphyses included bone mineral density (BMD), bone volume/total volume (BV/TV), trabecular thickness (Tb.Th), trabecular number (Tb.N), and trabecular separation (Tb Sp). (*E*) von Kossa-stained vertebral sections from vehicle- or irisin-injected mice, together with trabecular bone parameters as in *D*. Data are presented as mean ± SEM. Statistics: Unpaired Student's *t* test, $n = 5$–7 mice per group. $^*P \leq 0.05$, or shown in *D*.

Results

We have previously reported that conditioned medium from cultures of myoblasts harvested from mice postexercise was able to enhance osteoblast differentiation in vitro (17). This observation suggested that the newly discovered myokine irisin could be a potential candidate for muscle-osteoblast connectivity. We therefore injected young male mice with r-irisin (100 μg kg^{-1}) or vehicle once a week for 4 wk. X-ray imaging of intact animals showed increased radiodensity of femora and tibia of irisin-treated mice compared with those treated with vehicle (Fig. 1*A*). Tibiae were particularly radiodense at both midshaft and metaphyseal regions (arrows).

Micro-CT of the tibial midshaft showed a marked effect on cortical, but not on trabecular bone (Fig. 1 *B* and *C*). To allow for the determination of cortical tissue mineral density (TMD-Cortical) by converting grayscale to mineral density values, we used a density calibration phantom containing a hydroxyapatite standard. TMD-Cortical was higher in r-irisin–treated mice compared with vehicle controls (Fig. 1*D*). This difference was accompanied by an increase in cortical bone surface (Fig. 1*D*). Qualitative observations of tibia size, noted in micro-CT images (Fig. 1*B*), were confirmed by measuring bone perimeter (Pm). The latter was also higher in r-irisin–injected compared with vehicle-treated control mice (Fig. 1*D*). There were no differences in cortical thickness (Ct.Th). However, consistent with the increased Ct.Pm, both total cross-sectional area (Tt.Area) and marrow area (Ma.Area), were increased. These data are consistent with altered geometry of long bones.

Polar moment of inertia (pMOI), which is a quantity used to predict an object with an invariant circular cross-section, such as cortical bone, to resist torsion, was calculated as $J = (R_o^4 - R_i^4)\pi/2$, with R_o and R_i being radii of the periosteal and endosteal surfaces, respectively (18). Of note is that, as J is a function of the fourth power of difference in radii, any such difference is expected to have a large effect on pMOI. Expectedly, therefore, r-irisin–treated mice exhibited a profound ∼19% increase in pMOI ($P \leq 0.01$) compared with vehicle-treated controls (Fig. 1*D*). Consistent with this, the three point bending test demonstrated a significant increase in bending strength and force at peak (Fig. 2*A*).

Very interestingly, and in stark contrast to any other known therapy, r-irisin did not induce a change in trabecular bone at the proximal tibia (Fig. 1 *C* and *D*). Microstructural parameters, such as bone mineral density (BMD), bone volume/total, volume (BV/TV), trabecular number (Tb.N), thickness (Tb.Th), and Tb.Sp remained unchanged in r-irisin–treated compared with control mice (Fig. 1*D*). This remarkable finding indicated that irisin had a selective anabolic action on the cortical component of a long bone, essentially sparing its trabecular, metaphyseal component. Absence of an action of r-irisin on trabecular bone was further confirmed through histomorphometry of vertebral bodies (Fig. 1*E*).

Dynamic histomorphometry of the tibial cortical bone using timed injections of xylelol orange and calcein showed a significant increase in bone formation parameters, including bone formation rate (BFR) and mineral apposition rate (MFR) (Fig. 2*B*). Of note is the visible increase in osteoid (unmineralized bone) in Fig. 2*C*, which is again consistent with increased bone formation. Also consistent is an absolute increase in osteoblast numbers (Fig. 2*C*). In contrast, osteoclast numbers were significantly lower in the r-irisin–treated group (Fig. 2*D*). Thus, although the primary action of r-irisin is to stimulate bone formation, the inhibition of osteoclastic bone resorption in parallel also likely contributes to the increase in bone strength.

Irisin is known to activate the browning response in WAT, when injected daily at a dose of 500 μg kg^{-1} for 14 d (19, 20). We therefore chose a substantially lower dose of r-irisin (100 μg kg^{-1}, weekly injections) to determine whether or not the skeletal action of irisin was dependent on the expansion of inducible BAT (iBAT). Our cumulative weekly r-irisin dose was therefore 35-fold lower than that used to induce browning (100 μg kg^{-1} versus 3,500 μg kg^{-1} per mouse per week). Mice treated with r-irisin did not display a difference in tissue weight/body weight of either interscapular BAT or inguinal WAT (iWAT) (Fig. 3*A*). An absent browning response with 100 μg kg^{-1} r-irisin was also consistent with unchanged uncoupling protein 1 (*Ucp1*) expression in BAT and iWAT (Fig. 3*B*). Furthermore, there was no difference in morphology of iWAT adipocytes from r-irisin–treated and control mice (Fig. 3*C*). Additionally, no BAT-like phenotype was noted in r-irisin–injected mice (Fig. 3*C*).

To study actions of r-irisin on peroxisome proliferator-activated receptor-γ (PPARγ), the transcription factor that regulates adipogenesis, we analyzed marrow isolated from long bones of irisin-treated mice. *Pparγ* mRNA was not changed upon r-irisin injection, suggesting that r-irisin did not shift mesenchymal stem cell commitment toward an adipocyte lineage (Fig. 3*D*). Instead, there was a notable increase in marrow activating transcription factor 4 (*Atf4*) mRNA expression, indicating enhanced precursor differentiation toward an osteoblast lineage (Fig. 3*D*). Consistent with increased osteoblastic bone formation, we found a strong induction of secreted phosphoprotein 1 (osteopontin, *Spp1*) mRNA

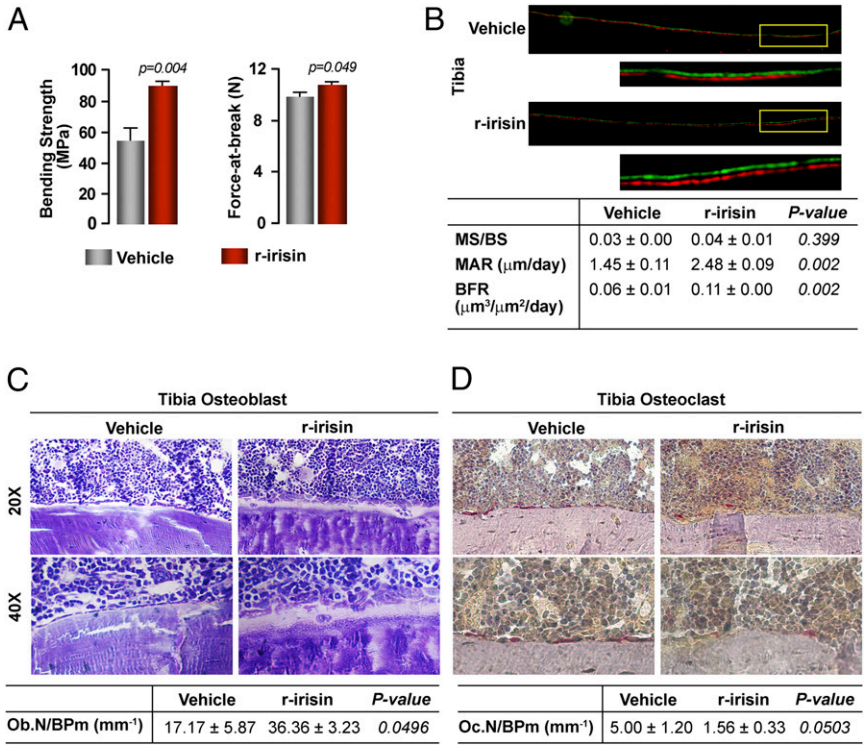

	Vehicle	r-irisin	*P-value*
MS/BS	0.03 ± 0.00	0.04 ± 0.01	*0.399*
MAR (μm/day)	1.45 ± 0.11	2.48 ± 0.09	*0.002*
BFR ($\mu m^3/\mu m^2$/day)	0.06 ± 0.01	0.11 ± 0.00	*0.002*

	Vehicle	r-irisin	*P-value*
Ob.N/BPm (mm^{-1})	17.17 ± 5.87	36.36 ± 3.23	*0.0496*

	Vehicle	r-irisin	*P-value*
Oc.N/BPm (mm^{-1})	5.00 ± 1.20	1.56 ± 0.33	*0.0503*

Fig. 2. Low-dose r-irisin increases bone strength by stimulating bone formation. (*A*) Three-point bending test on tibia from mice treated with vehicle or low-dose r-irisin (100 μg kg^{-1} per week for 28 d, mice killed 24 h after last dose). Bending strength and force-at-break are noted. (*B*) Dynamic histomorphometry on tibial sections following timed injections (2 and 7 d before sacrifice) of xylelol orange and calcein, respectively. Representative images are shown, together with calculated indices of bone formation, including mineralized surface/total bone surface (MS/BS), mineral apposition rate (MAR), and bone formation rate (BFR). Also shown are representative images of toluidine blue-stained osteoblasts (*C*) and tartrate-resistant acid phosphatase-stained osteoclasts (*D*) in tibial diaphyseal sections, together with cell counts (Ob and Oc, respectively) per bone perimeter (BPm). Data are presented as mean ± SEM. Statistics: Unpaired Student's *t* test, $n = 4–5$ mice per group. *P* values as shown.

expression in whole tibia (Fig. 3*E*). Conversely, mRNA expression for *Sost*, a natural inhibitor of bone formation, was reduced in tibiae from r-irisin–treated mice (Fig. 3*E*). Immunofluorescence also revealed more abundant Spp1 immunolabeling, quantitated as Spp1/BS, in the endosteal and periosteal surfaces of cortical bone from mice treated with r-irisin compared with control mice (Fig. 3*F*).

We tested the effect of r-irisin on the differentiation of bone marrow stromal cells in the presence of ascorbic acid and β-glycerophosphate. Incubation with r-irisin (100 ng/mL) significantly increased in the number of Alp-positive (Cfu-f) and von Kossa-positive (mineralized) colonies (Cfu-ob), and up-regulated *Spp1* and Bone gamma-carboxyglutamic acid-containing protein (*Bglap*) mRNA expression at 10 d (Fig. 4 *A–C*). In the short term, there was a rapid up-regulation, within 3 h, of *Atf4* mRNA, suggesting a key role for Atf4 in mediating irisin-induced osteoblast differentiation (Fig. 4*D*). Interestingly, there was no change in *Runt-related transcription factor-2* (*Runx2*) mRNA expression at 3 or 8 h of r-irisin treatment (Fig. 4*D*). However, further incubation for 48 h induced the up-regulation of *Runx2* and Sp7 transcription factor (osterix, *Sp7*) mRNA, together with the Wnt signal-related genes low density lipoprotein receptor-related protein 5 (*Lrp5*) and *β-catenin* (Fig. 4*E*). The up-regulation of *Atf4*, *Runx2*, and *Sp7* was consistent with the global enhancement of expression of early differentiation genes, including alkaline phosphatase (*Alp*) and collagen, type I, alpha 1 (*Col1a1*) mRNA (Fig. 4*E*). Late genes, such as *Bglap*, integrin-binding sialoprotein (*Ibsp*), and *Spp1* remained unchanged at 48 h (Fig. 4*E*). Finally, whereas a receptor for irisin has not yet been identified, it was clear that irisin targeted the osteoblast directly, and in doing so, stimulated Erk phosphorylation with 5 min of application (Fig. 4*F*).

Finally, we explored whether irisin was produced at locations other than muscle. Quantitative PCR (qPCR) showed that, whereas muscle was the major site for *Fndc5* expression, the molecule was also produced in bone and brain tissue, albeit to a significantly lesser extent (Fig. 5*A*). Fat tissue, namely iWAT and eWAT, contributed minimally to irisin production (Fig. 5*A*); this is in line with previous studies (21). Using a specific Fndc5 antibody (Fig. S1), we found a modest increase in Fndc5 immunofluorescence in muscle fibers from r-irisin–injected mice compared with vehicle-injected mice (Fig. 5*B*). Irisin-induction of *Fndc5* mRNA expression was confirmed in C2C12 myoblasts (Fig. 5*C*), further suggesting that irisin signaling could perhaps be amplified through an autocrine action.

Discussion

Here, we report that the myokine irisin, when injected at cumulative weekly dose of 100 μg kg^{-1}, profoundly stimulates cortical bone mass and bone strength in mice but spares the trabecular compartment. This action is accompanied by dramatically increased osteoblastic bone formation, up-regulated pro-osteoblastic genes, and diminished osteoblast inhibitors, such as *Sost*. Importantly, at this dose, irisin does not induce browning of WAT, nor does it change the levels of molecular markers of browning (*Ucp1*) or adipogenesis (*Pparγ*), a phenomenon classically noted at a 35-fold higher cumulative dose (11). We hypothesize, therefore, that irisin is fundamental to muscle–bone communication, and likely translates the well known skeletal anabolic action of exercise by directly stimulating new bone synthesis by osteoblasts.

It is clear that r-irisin injection not only alters cortical bone density, but also bone geometry typified by an increase in periosteal perimeter. This effect likely arises from greater bone formation at the periosteal surface, a notion consistent with enhanced

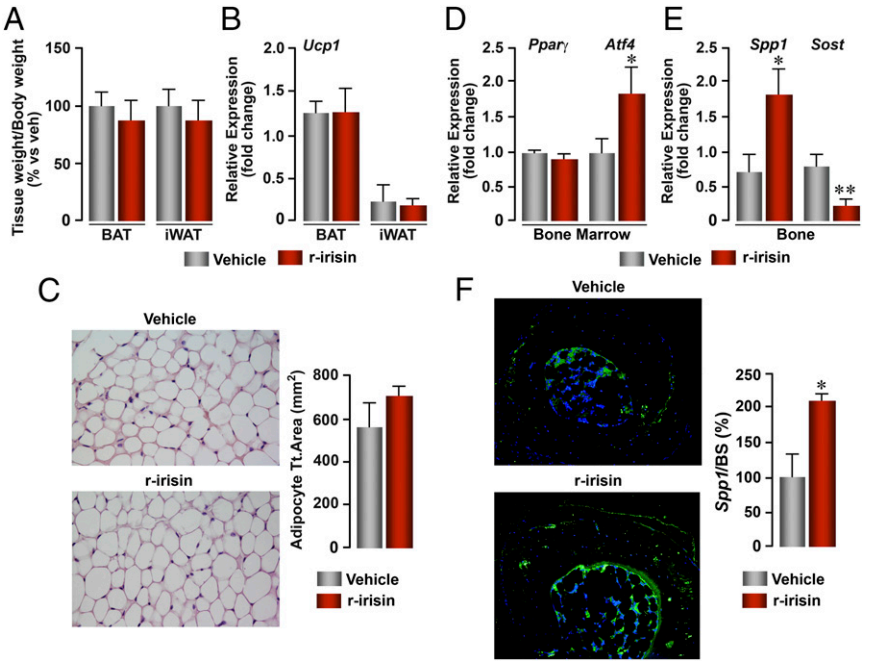

Fig. 3. Low-dose r-irisin modulates osteoblast gene expression in vivo without causing a browning response. (*A*) Mice injected with low-dose r-irisin (100 μg kg^{-1} per week for 28 d, mice killed 24 h after last dose) do not display a difference in tissue weight/body weight of interscapular brown adipose tissue (BAT) and inguinal white adipose tissue (iWAT). (*B*) r-irisin injection also does not affect uncoupling protein-1 (*Ucp1*) mRNA expression in BAT or iWAT. (*C*) Photomicrographs of hematoxylin and eosin stained sections of iWAT from vehicle- and r-irisin–injected mice (magnification: 40×), showing no difference. (*D*) *Pparγ* and *Atf4* mRNA expression (qPCR) in whole bone marrow isolated from tibiae of vehicle- or r-irisin–injected mice. (*E*) *Spp1* and *Sost* mRNA expression (qPCR) in whole tibia (depleted of bone marrow) harvested from vehicle- or r-irisin–injected mice. (*F*) Fluorescent micrographs of metatarsal sections of vehicle- or r-irisin–injected mice immunolabeled for *Spp1* (green; nuclei labeled blue; magnification: 20×). *Spp1* positivity was measured as percentage of green fluorescence area/total bone area (*Spp1*/BS). Data are presented as mean ± SEM. Statistics: Unpaired Student's *t* test, $n = 4$–5 mice per group. $^*P \leq 0.05$.

Spp1 immunostaining. As a consequence, pMOI, an index of long bone resistance to torsion, and bending strength are significantly increased. Both BMD increases and geometry improvements are known to underlie enhanced bone strength (22–24). Specifically, by distributing bone mass away from the center, enlarged bone perimeter and cross-sectional area both contribute to increased pMOI and resistance to bending. The effect of r-irisin, essentially mimicking the effect of mechanotransduction (25–27), thus allows bone to become structurally more efficient for bending and torsion. Indeed, both mouse (28–30) and rat (31–34) models have collectively shown positive associations between exercise and increased bone size and bone mass.

Despite this profound proosteoblastic action on cortical bone, r-irisin did not induce a change in trabecular compartment of the same bone. There was no change in thickness, number, and separation of trabeculae in r-irisin–treated compared with control mice. Although it remains unclear why osteoblasts at cortical surfaces will behave differently from those synthesizing trabecular bone, our observation is in line with data indicating greater sensitivity of cortical bone to anabolic factors released by muscle (26, 27, 35). The selective action of r-irisin on cortical bone is likely to be related to the different functionalities of cortical and trabecular bone. Admittedly speculative, it is possible that points of maximal biomechanical stress in cortical bone are irisin targets, as is obvious in Fig. 1*A*.

The bone-forming action of irisin is mediated initially by Atf4, followed by *Runx2* expression, which, in turn, triggers a global osteogenesis gene program. Although the mechanism of this action needs further study, it seems clear that it is receptor-mediated, in that Erk phosphorylation is stimulated within 5 min of r-irisin application. Furthermore, in in vivo studies, we show downstream effects of r-irisin on two osteoblast genes that are known to be responsive to mechanostimulation, namely *Spp1* and *Sost*. This effect is consistent with the observation that $Spp1^{-/-}$ mice are resistant to unloading-induced bone loss (36, 37). *Spp1* expression is increased on cortical surfaces upon 4 wk of r-irisin treatment in vivo. However, r-irisin does not enhance *Spp1* expression in 48-h cultures, likely because of our use of yet-undifferentiated marrow stromal cells. We therefore speculate that *Spp1* up-regulation by irisin may underlie its role in transducing the effects of mechanical stimulation (38, 39).

In contrast to *Spp1*, r-irisin injections down-regulates sclerostin, a Wnt/β-catenin pathway inhibitor known to negatively regulate bone formation (40–42). Load-induced decreases in *Sost* expression have been associated with increased bone formation (43). Furthermore, and interestingly, serum irisin levels in people are inversely correlated with serum sclerostin levels independently of age or sex (44). There is also an inverse correlation between serum irisin levels and vertebral fragility fractures in postmenopausal women (45, 46). In contrast, irisin levels in athletes positively correlate with BMD (47). In addition, we provide in vitro evidence for an early up-regulation of *Lrp5* and *β-catenin*, both of which may play key roles in stimulating Wnt signaling.

Irisin was discovered as a myokine that triggered the transdifferentiation of white to brown adipose tissue in mice (11). Notably, at a dose of 500 μg kg^{-1} daily (3,500 μg kg^{-1} per week), r-irisin increased *Ucp1* expression and reduced body weight. However, because BAT, particularly iBAT, can be beneficial to the skeleton (20, 48, 49), it was imperative that we exclude indirect effects of irisin on the skeleton exerted through iBAT. We therefore used a 35-fold lower cumulative weekly dose of r-irisin than that used previously to induce browning (19). At this dose, r-irisin did not affect WAT-to-BAT conversion, essentially ruling out an indirect action of r-irisin on bone mass via adipose tissue browning. Equally importantly, it suggested that the skeleton was more sensitive to irisin than fat cells; this is not inconceivable, as the skeleton is more primitive evolutionarily. However, it is quite

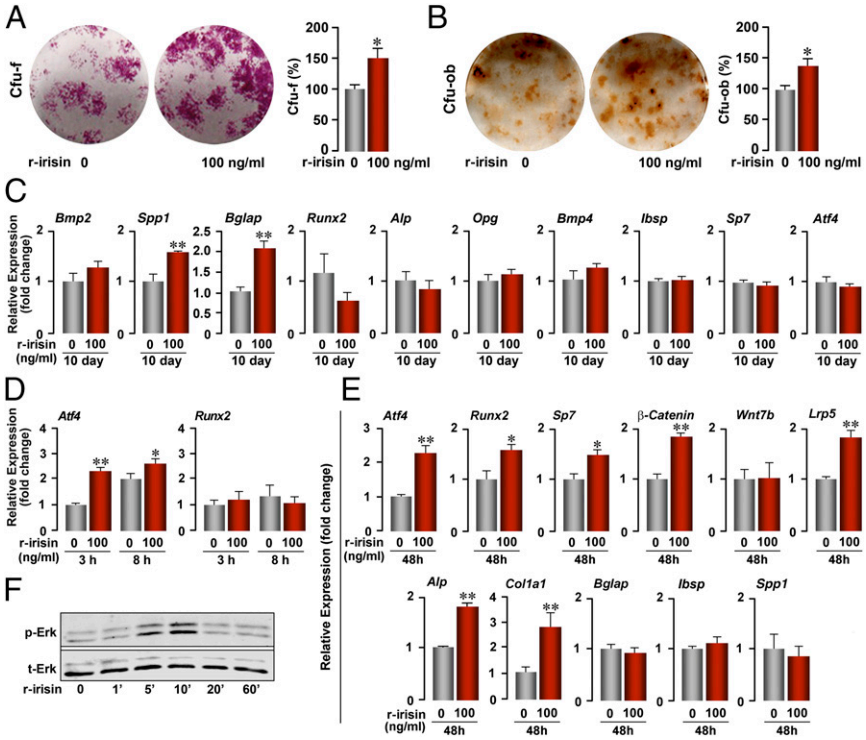

Fig. 4. Recombinant irisin enhances osteoblast differentiation. Bone marrow stromal cells were grown in osteoblast differentiation medium in the presence of r-irisin (100 ng/mL). The percentage of alkaline phosphatase-positive colonies (10 d) (*A*) and von Kossa-positive mineralized colonies (21 d) (*B*) were calculated versus untreated cultures. Representative wells are shown. (*C*) mRNA expression levels of osteoblast marker genes (*Bmp2*, *Spp1*, *Bglap*, *Runx2*, *Alp*, *Opg*, *Bmp4*, *Ibsp*, *Sp7*, and *Atf4*) were assayed (qPCR) after 10-d culture with r-irisin. Osteoblast transcription regulators (*Atf4*, *Runx2*, and *Sp7*) and osteogenesis genes (*Alp*, *Col1a1*, *Bglap*, *Ibsp*, *Spp1*, *Lrp5*, *Wnt7b*, and *β-catenin*) were evaluated (qPCR) following culture with r-irisin for 3, 8 (*D*), or 48 h (*E*). (*F*) Western immunoblotting showing Erk phosphorylation (p-Erk) triggered by r-irisin (100 ng/mL) in osteoblast cultures. Data are presented as mean ± SEM. Statistics: Unpaired Student's *t* test. $*P \leq 0.05$; $**P \leq 0.01$.

possible that higher doses of r-irisin, which affect BAT expansion (11), may have anabolic actions on both cortical and trabecular bone, particularly as BAT is anabolic to the skeleton (20).

Taken together, our data add another milestone to the biological evidence supporting the tight relationship between skeletal muscle tissue and the skeleton. We also report a previously unidentified role for irisin, likely in mediating muscle–bone connectivity. This connection could shed further light on how exercise triggers a skeletal anabolic response, and in particular, how age-related decrements in physical activity may impact irisin production. Whether these effects in mice recapitulate human physiology needs further study, particularly as the pattern of expression of irisin in humans is somewhat unclear due to an unusual ATA start codon of the human *FNDC5* gene (50–52). Nonetheless, the therapeutic potential of r-irisin analogs stems from the possibility of treating osteoporosis, sarcopenia, and metabolic syndrome all at once.

Methods

All procedures were performed on 2-mo-old C57BL/6 male mice in protocols approved by the Institutional Animal Care and Use Committees. Harvested femur and tibia were imaged by contact X-ray radiography (VistaScan Combi View, Durr Dental) at a setting of 60 kV, 8 mA, and 2.5 s, and X-ray films were digitized for image analysis. For micro-CT, images were acquired using Bruker Skyscan 1172 (voxel size = 6 μm^3; peak tube potential = 59 kV, X-ray intensity = 167 μA, ring artifact correction = 10, beam hardening correction = 60%). Three hydroxyapatite (HA) phantoms were used for calibration to compute volumetric BMD. Structural indices were calculated using the Skyscan CT Analyzer (CTAn) software (Bruker). For cortical bone properties, tibiae were scanned at the middiaphysis starting 5.5 mm from proximal tibial condyles and extending for 100 6-μm slices (0.6 mm). For trabecular bone, tibiae were scanned starting 1.9 mm from the proximal tibial condyles, just distal to the growth plate, in the direction of the metaphysis, and extending for 100 slices (0.6 mm). Calculated cortical and trabecular parameters are noted in Fig. 1*D*. Dynamic histomorphometry was performed as described (53). The three-point bending test was carried out according to a previous protocol (54).

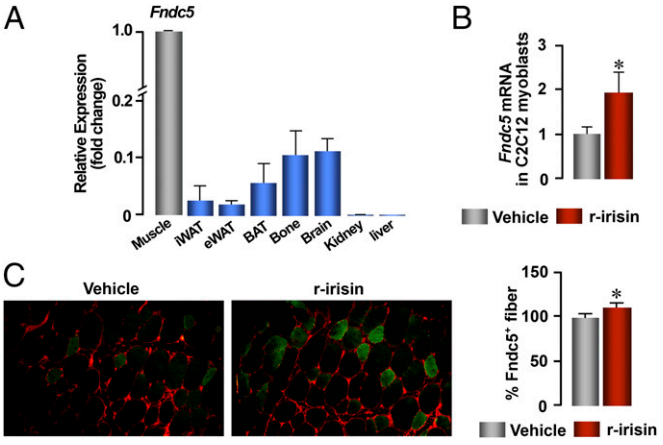

Fig. 5. Irisin expression beyond muscle. (*A*) Fibronectin type III domain-containing protein-5 (*Fndc5*) mRNA levels in different tissues, namely muscle, iWAT (inguinal white adipose tissue), eWAT (epididymal white adipose tissue), BAT (brown adipose tissue), bone, brain, kidney, and liver (qPCR). (*B*) Immunofluorescence micrograph of muscle fibers from mice injected with vehicle or r-irisin (100 μg kg^{-1} per week for 28 d) costained for Fndc5 (green) and dystrophin (red) (Magnification: 20×). Fndc5-positive fibers were quantitated as percentage of green fluorescent fibers/total fibers. (*C*) Effect of r-irisin on *Fndc5* mRNA in C2C12 myoblasts (qPCR). Data are presented as mean ± SEM. Statistics: Unpaired Student's *t* test, $n = 4–5$ mice per group. $*P \leq 0.05$.

Primary osteoblast culture, immunoblotting and qPCR were performed as described (17). Cfu-f and Cfu-ob were determined by alkaline phosphatase (day 10) and von Kossa (day 21) labeling, respectively. Anti-pErk and anti-tErk antibodies were purchased from Santa Cruz. Analyses were performed using unpaired Student's *t* test for significant differences at $P < 0.05$. For immunohistochemistry, vastus lateralis muscles were excised from the quadriceps, fixed and embedded in paraffin. Histological sections (5 μm thick) were cut and incubated with primary antibodies against dystrophin and Fndc5 (Abcam). Fluorescent-labeled goat anti-mouse or anti-rabbit secondary antibodies (Alexa-555 and Alexa-488, respectively; Invitrogen) were used for detection. Specificity of the antibody was assessed by Western immunoblotting (Fig. S1). Recombinant irisin was purchased from Adipogen (AG-40B-0103).

ACKNOWLEDGMENTS. We thank Prof. Alberta Zallone for invaluable intellectual input. This work was supported in part by the European Research In Space And Terrestrial Osteoporosis (ERISTO) grant (to M.G.); Italian Ministry of Education, Universities and Research (MIUR) Grant ex60% (to M.G.); the Italian Society for Osteoporosis, Mineral Metabolism and Skeleton Diseases (SIOMMMS) grant (to G.C.); MIUR Grant PRIN-2011 (to S. Cinti); and National Institutes of Health Grants AG40132 (to M.Z.), AG23176 (to M.Z.), AR65932 (to M.Z.), and AR67066 (to M.Z.).

1. Dunstan D (2011) Diabetes: Exercise and T2DM-move muscles more often! *Nat Rev Endocrinol* 7(4):189–190.
2. Baxter-Jones AD, Kontulainen SA, Faulkner RA, Bailey DA (2008) A longitudinal study of the relationship of physical activity to bone mineral accrual from adolescence to young adulthood. *Bone* 43(6):1101–1107.
3. Andreoli A, Celi M, Volpe SL, Sorge R, Tarantino U (2012) Long-term effect of exercise on bone mineral density and body composition in post-menopausal ex-elite athletes: A retrospective study. *Eur J Clin Nutr* 66(1):69–74.
4. Epstein S, Inzerillo AM, Caminis J, Zaidi M (2003) Disorders associated with acute rapid and severe bone loss. *J Bone Miner Res* 18(12):2083–2094.
5. Keyak JH, Koyama AK, LeBlanc A, Lu Y, Lang TF (2009) Reduction in proximal femoral strength due to long-duration spaceflight. *Bone* 44(3):449–453.
6. Oppl B, et al. (2014) Low bone mineral density and fragility fractures in permanent vegetative state patients. *J Bone Miner Res* 29(5):1096–1100.
7. Clarke BL, Khosla S (2010) Physiology of bone loss. *Radiol Clin North Am* 48(3):483–495.
8. Cardozo CP, et al. (2010) Nandrolone slows hindlimb bone loss in a rat model of bone loss due to denervation. *Ann N Y Acad Sci* 1192:303–306.
9. Sun L, et al. (2013) Anabolic steroids reduce spinal cord injury-related bone loss in rats associated with increased Wnt signaling. *J Spinal Cord Med* 36(6):616–622.
10. Qin W, et al. (2013) The central nervous system (CNS)-independent anti-bone-resorptive activity of muscle contraction and the underlying molecular and cellular signatures. *J Biol Chem* 288(19):13511–13521.
11. Boström P, et al. (2012) A PGC1-α-dependent myokine that drives brown-fat-like development of white fat and thermogenesis. *Nature* 481(7382):463–468.
12. Himms-Hagen J, et al. (2000) Multilocular fat cells in WAT of CL-316243-treated rats derive directly from white adipocytes. *Am J Physiol Cell Physiol* 279(3):C670–C681.
13. Barbatelli G, et al. (2010) The emergence of cold-induced brown adipocytes in mouse white fat depots is determined predominantly by white to brown adipocyte transdifferentiation. *Am J Physiol Endocrinol Metab* 298(6):E1244–E1253.
14. Rosen ED, Spiegelman BM (2014) What we talk about when we talk about fat. *Cell* 156(1-2):20–44.
15. Cinti S (2009) Transdifferentiation properties of adipocytes in the adipose organ. *Am J Physiol Endocrinol Metab* 297(5):E977–E986.
16. Waldén TB, Hansen IR, Timmons JA, Cannon B, Nedergaard J (2012) Recruited vs. nonrecruited molecular signatures of brown, "brite," and white adipose tissues. *Am J Physiol Endocrinol Metab* 302(1):E19–E31.
17. Colaianni G, et al. (2014) Irisin enhances osteoblast differentiation in vitro. *Int J Endocrinol* 2014:902186.
18. Ugural A, Fenster S (1995) Advanced Strength and Applied Elasticity (Prentice-Hall, Englewood Cliffs, NJ), 3rd Ed.
19. Zhang Y, et al. (2014) Irisin stimulates browning of white adipocytes through mitogen-activated protein kinase p38 MAP kinase and ERK MAP kinase signaling. *Diabetes* 63(2):514–525.
20. Rahman S, et al. (2013) Inducible brown adipose tissue, or beige fat, is anabolic for the skeleton. *Endocrinology* 154(8):2687–2701.
21. Roca-Rivada A, et al. (2013) FNDC5/irisin is not only a myokine but also an adipokine. *PLoS One* 8(4):e60563.
22. Fonseca H, Moreira-Gonçalves D, Coriolano HJ, Duarte JA (2014) Bone quality: The determinants of bone strength and fragility. *Sports Med* 44(1):37–53.
23. Seeman E (2002) An exercise in geometry. *J Bone Miner Res* 17(3):373–380.
24. Orwoll ES (2003) Toward an expanded understanding of the role of the periosteum in skeletal health. *J Bone Miner Res* 18(6):949–954.
25. Lieberman DE, Pearson OM, Polk JD, Demes B, Crompton AW (2003) Optimization of bone growth and remodeling in response to loading in tapered mammalian limbs. *J Exp Biol* 206(Pt 18):3125–3138.
26. Ducher G, Bass SL, Saxon L, Daly RM (2011) Effects of repetitive loading on the growth-induced changes in bone mass and cortical bone geometry: A 12-month study in pre/peri- and postmenarcheal tennis players. *J Bone Miner Res* 26(6):1321–1329.
27. Johannesdottir F, et al. (2012) Mid-thigh cortical bone structural parameters, muscle mass and strength, and association with lower limb fractures in older men and women (AGES-Reykjavik Study). *Calcif Tissue Int* 90(5):354–364.
28. Mori T, et al. (2003) Climbing exercise increases bone mass and trabecular bone turnover through transient regulation of marrow osteogenic and osteoclastogenic potentials in mice. *J Bone Miner Res* 18(11):2002–2009.
29. Wu J, Wang XX, Higuchi M, Yamada K, Ishimi Y (2004) High bone mass gained by exercise in growing male mice is increased by subsequent reduced exercise. *J Appl Physiol* 97(3):806–810.
30. Hoshi A, Watanabe H, Chiba M, Inaba Y (1998) Bone density and mechanical properties in femoral bone of swim loaded aged mice. *Biomed Environ Sci* 11(3):243–250.
31. Umemura Y, Ishiko T, Yamauchi T, Kurono M, Mashiko S (1997) Five jumps per day increase bone mass and breaking force in rats. *J Bone Miner Res* 12(9):1480–1485.
32. Iwamoto J, Yeh JK, Aloia JF (2000) Effect of deconditioning on cortical and cancellous bone growth in the exercise trained young rats. *J Bone Miner Res* 15(9):1842–1849.
33. Notomi T, et al. (2001) Effects of tower climbing exercise on bone mass, strength, and turnover in growing rats. *J Bone Miner Res* 16(1):166–174.
34. Huang TH, et al. (2003) Effects of different exercise modes on mineralization, structure, and biomechanical properties of growing bone. *J Appl Physiol* 95(1):300–307.
35. Elkasrawy MN, Hamrick MW (2010) Myostatin (GDF-8) as a key factor linking muscle mass and bone structure. *J Musculoskelet Neuronal Interact* 10(1):56–63.
36. Toma CD, Ashkar S, Gray ML, Schaffer JL, Gerstenfeld LC (1997) Signal transduction of mechanical stimuli is dependent on microfilament integrity: Identification of osteopontin as a mechanically induced gene in osteoblasts. *J Bone Miner Res* 12(10):1626–1636.
37. Ishijima M, et al. (2007) Osteopontin is required for mechanical stress-dependent signals to bone marrow cells. *J Endocrinol* 193(2):235–243.
38. Harter LV, Hruska KA, Duncan RL (1995) Human osteoblast-like cells respond to mechanical strain with increased bone matrix protein production independent of hormonal regulation. *Endocrinology* 136(2):528–535.
39. Kubota T, et al. (1993) Influence of an intermittent compressive force on matrix protein expression by ROS 17/2.8 cells, with selective stimulation of osteopontin. *Arch Oral Biol* 38(1):23–30.
40. Paszty C, Turner CH, Robinson MK (2010) Sclerostin: A gem from the genome leads to bone-building antibodies. *J Bone Miner Res* 25(9):1897–1904.
41. Lin C, et al. (2009) Sclerostin mediates bone response to mechanical unloading through antagonizing Wnt/beta-catenin signaling. *J Bone Miner Res* 24(10):1651–1661.
42. Li X, et al. (2008) Targeted deletion of the sclerostin gene in mice results in increased bone formation and bone strength. *J Bone Miner Res* 23(6):860–869.
43. Robling AG, et al. (2008) Mechanical stimulation of bone in vivo reduces osteocyte expression of Sost/sclerostin. *J Biol Chem* 283(9):5866–5875.
44. Klangjareonchai T, et al. (2014) Circulating sclerostin and irisin are related and interact with gender to influence adiposity in adults with prediabetes. *Int J Endocrinol* 2014:261545.
45. Palermo A, et al. (2015) Irisin is associated with osteoporotic fractures independently of bone mineral density, body composition or daily physical activity. *Clin Endocrinol (Oxf)* 82(4):615–619.
46. Anastasilakis AD, et al. (2014) Circulating irisin is associated with osteoporotic fractures in postmenopausal women with low bone mass but is not affected by either teriparatide or denosumab treatment for 3 months. *Osteoporos Int* 25(5):1633–1642.
47. Singhal V, et al. (2014) Irisin levels are lower in young amenorrheic athletes compared with eumenorrheic athletes and non-athletes and are associated with bone density and strength estimates. *PLoS One* 9(6):e100218.
48. Motyl KJ, et al. (2013) Altered thermogenesis and impaired bone remodeling in Misty mice. *J Bone Miner Res* 28(9):1885–1897.
49. Bredella MA, et al. (2012) Young women with cold-activated brown adipose tissue have higher bone mineral density and lower Pref-1 than women without brown adipose tissue: A study in women with anorexia nervosa, women recovered from anorexia nervosa, and normal-weight women. *J Clin Endocrinol Metab* 97(4):E584–E590.
50. Raschke S, et al. (2013) Evidence against a beneficial effect of irisin in humans. *PLoS One* 8(9):e73680.
51. Albrecht E, et al. (2015) Irisin - a myth rather than an exercise-inducible myokine. *Sci Rep* 5:8889.
52. Ivanov IP, Firth AE, Michel AM, Atkins JF, Baranov PV (2011) Identification of evolutionarily conserved non-AUG-initiated N-terminal extensions in human coding sequences. *Nucleic Acids Res* 39(10):4220–4234.
53. Zhu LL, et al. (2012) Blocking antibody to the β-subunit of FSH prevents bone loss by inhibiting bone resorption and stimulating bone synthesis. *Proc Natl Acad Sci USA* 109(36):14574–14579.
54. Westbroek I, et al. (2007) Long-term fluoxetine administration does not result in major changes in bone architecture and strength in growing rats. *J Cell Biochem* 101(2):360–368.

Supporting Information

Colaianni et al. 10.1073/pnas.1516622112

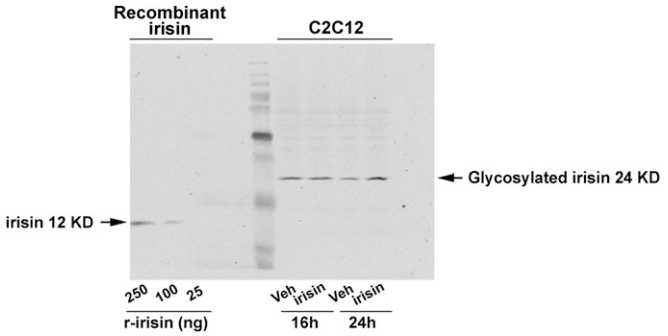

Fig. S1. Specificity of the anti-irisin antibody (Abcam). Western immunoblot showing that the antibody not only recognized recombinant irisin (ng), but also, in C2C12 myoblast supernatants, its high-molecular-weight glycosylated form.